The effect of growth rate on the three-dimensional orientation of vascular canals in the cortical bone of broiler chickens

Isaac V. Pratt (iD) and David M. L. Cooper

Department of Anatomy & Cell Biology, University of Saskatchewan, Saskatoon, SK, Canada

Abstract

Vascular canals in cortical bone during growth and development typically show an anisotropic pattern with canals falling into three main categories: circumferential, radial, and longitudinal. Two major hypotheses attempt to explain the preferred orientations in bone: that vascular canal orientation is optimized to resist a predominant strain direction from functional loading, or that it reflects growth requirements and velocity. We use a controlled growth experiment in broiler chickens to investigate the effect of growth rate on vascular canal orientation. Using feed restriction we set up a fast growing control group and a slow growing restricted group. We compared the microstructure in the humerus and the femur at 42 days of age using synchrotron micro-computed tomography (micro-CT), a three-dimensional (3D) method that visualizes the full canal network. We measured the 3D orientation of each canal in the whole cross-section of the bone cortex using a set of custom IMAGEJ scripts. Using these orientations we compute laminar, radial, and longitudinal indices that measure the proportion of circumferential, radial, and longitudinal canals, by unit of length, in the cortex. Following previous studies we hypothesized that vascular canal orientation is related to growth, with radial canals linked to a faster growth rate and related to functional loading through a high laminar index in flight bones which reflects torsional loading resulting from active flight. The control group had final body weights that were nearly twice the final weights of the restricted group and higher absolute growth rates. We found consistent patterns in the comparison between the humerus and the femur in both groups, with the humerus having higher laminar and longitudinal indices, and a lower radial index than the femur. The control group had higher radial indices and lower laminar and longitudinal indices in both the humerus and the femur than the restricted group. The higher radial indices in our control group point to a link between radial canals and faster growth, and between laminar canals and slower growth, while the higher laminar indices in the humerus point to a link between circumferential canals and torsional loading. Overall, our results indicate that the orientation of the cortical canal network in a bone is the consequence of a complex interaction between the growth rate of that bone and functional loading environment.

Key words: Micro-CT; bone vascularity; laminar bone; bone microstructure.

Introduction

Cortical bone is a major component of the strength of a bone. In particular, the porosity within cortical bone is important in developing the asymmetrical strength required by each bone's particular functional requirements (Currey, 2002; Ammann & Rizzoli, 2003; Cooper et al. 2016).

The cortical canal network forms initially during the primary formation of a bone. In fibrolamellar bone, vascular spaces incorporated from the periosteum are closed in by deposition of layers of lamellar bone. Over time these spaces are filled in, leaving a network of connected primary canals, or primary osteons (Maggiano, 2012). In humans and most larger animals, bone is continually renewed through the turnover of bone tissue in a process known as remodeling. Remodeling bores new canals through bone which are then filled in with new 'secondary' bone, creating the structures known as secondary osteons.

The orientation of cortical canals, both primary and secondary, is a useful signal in bone microstructure, but its full etiology is not clear. In a long bone, the orientation of a

Correspondence

David M. L. Cooper, Department of Anatomy & Cell Biology, University of Saskatchewan, 2D01 Health Sciences Building, 107 Wiggins Rd., Saskatoon, SK S7N 5E5, Canada. E: dml.cooper@usask.ca

canal can be longitudinal (meaning parallel to the long axis of the bone), radial (oriented like rays emanating from the centroid, like spokes on a bicycle wheel), circumferential (meaning parallel to the circumference, like the orbit of a planet) or oblique (falling between the other categories) Measuring the proportion of one category of canal orientations to all the canals gives indices, the most common of which is the laminar index popularized by de Margerie et al. (2002) after de Ricqlès et al. (1991). de Margerie et al. (2002) defined the laminar index as the proportion of circumferential canal area to total canal area as measured in two-dimensional (2D) histological sections. Canal orientation is thought to be related to both functional loading and growth, with primary canals reflecting the situation during the initial growth phase and secondary canals reflecting later life periods. Secondary canals can yield more mixed signals; the loading experienced by a bone may change in later life and the remodeling process may not overwrite all canals from earlier life, so canals from a previous period can confound measurements.

A link between functional loading and canal orientation was proposed by Hert et al. (1994) and Petrtyl et al. (1996), who suggested that longitudinal canal orientations in the human femur optimized resistance to bending forces, and by de Margerie et al. (2002), who proposed that circumferential canals in mallard duck wing bones helped resist torsional forces created by flight and showed that mallards had a significantly higher laminar index in the wing bones than in the hindlimb bones. Evidence from rats (Britz et al. 2012) showed that a 6-month period of paralysis-induced disuse in a rat hindlimb drastically changes the canal orientation pattern in the tibia. de Margerie et al. (2002) also found no significant relation between canal orientation and bone growth rate in mallard long bones. de Margerie et al. (2004) suggested that radial canals have the lowest mechanical resistance to shear stress of all the canal orientations and circumferential canals the highest. We previously found a higher laminar index in the femur than the humerus in a comparative study of birds and bats (Pratt et al. 2018), a result that does not support a link between functional loading and canal orientation.

The other potentially significant factor relating to differences in canal orientation is growth rate. Studies in king penguin chicks (de Margerie et al. 2004) and in *Tyrannosaurus rex* (de Boef et al. 2007) found relations between growth rate and vascular canal orientation, with bone with more radial canals growing faster and bone with more circumferential canals (corresponding to a higher laminar index) growing slower. Skedros & Hunt (2004) found a significantly higher laminar index in adult turkey ulnae compared to sub-adult bones. They suggested that the increase in laminarity from sub-adult to adult may be caused by a change in loading history, from predominantly bending in the sub-adults to predominantly torsion in the adults, or by ontogenetic changes in growth rate. They believed that the

changes in growth rate may be the stronger factor, with lower growth rates in the adult bones linked to the higher laminar index.

The orientation of cortical canals has traditionally been measured using ground section histology but we here employ a more advanced method using micro-computed tomography (micro-CT). Micro-CT is ideal for measuring canal orientation, as it can visualize and measure the full 3D orientation of each canal in the vascular network of a bone (Pratt & Cooper, 2017), and measures bone and canal morphology in three dimensions (Cooper et al. 2003). Compared with histology, micro-CT is also less destructive to the sample and enables analysis of a much larger number of canals.

To help shed more light on the relation between growth rate and cortical canal orientation, we ran a controlled growth experiment using broiler chickens. Modern broiler chickens, including the strain used here, have undergone long-term selective breeding programs for faster growth and feed efficiency (Rawlinson et al. 2009) with modern broiler chicken growth rates 300% higher than those of ancestral birds (Knowles et al. 2008). These programs have been very successful, resulting in animals with very high growth rates which can be easily controlled through their diet (Williams et al. 2004) using feed-restriction techniques. Broiler chickens are used extensively as meat poultry and their rapid growth rate results in skeletal issues including frequent bone defects and leg fractures (Knowles et al. 2008; Pines & Reshef, 2014). Extremely fast growth in these animals may lead to bones that are weaker with lower stiffness, resistance to fracture, and bones that may have a lower ability to respond to mechanical loading (Rawlinson et al. 2009; Shim et al. 2012).

This study used two groups of broiler chickens: a control group fed *ad libitum*, and a feed-restricted group. Following Williams et al. (2004) we predicted that the control group would have a significantly higher growth rate than the restricted group. We used micro-CT to scan a mid-diaphyseal portion of the right femur and humerus from each individual and measured the full 3D cortical canal orientation in each bone. We then calculated a laminar, radial, and longitudinal index for each bone. Based on the previous evidence suggesting a link between faster growth and radial canal orientation, we predicted that the restricted group would contain a lower radial index than the control group, and a higher laminar index. We also hypothesized that the humerus would have a higher laminar index than the femur. This would support the idea that bones involved in flight exhibit laminar bone as an adaptation to torsional loading.

Materials and methods

We used 31 Ross 308 broiler chickens (Prairie Pride Natural Foods Ltd, Saskatoon, Canada) separated into two groups, an experimental group and a control group. The final number of chickens in the

experimental group was 16 and in the control group 15. This is a commercial strain of chickens that has been bred extensively for fast growth. We used male chickens because they have a higher natural growth rate than females. The chicks were treated with Vaxxitek (Merial Canada). We started with day-old chicks, which ensured control over the diet of the animals across their entire lifespan. We chose an endpoint of 42 days, a common end time point used in broiler chicken bone growth studies (Williams et al. 2000, 2004). By 37 days, areas of laminar bone have been observed in the tibiotarsus of broiler chickens (Leterrier & Nys, 1992), indicating that this time length is sufficient for laminar bone to develop. Micro-CT scans were taken of the mid-humerus and femur of each individual.

Animal ethics approval was granted by the University of Saskatchewan Animal Research Ethics Board of the University Committee on Animal Care and Supply (protocol 2015-0080) and by the Canadian Light Source.

Housing, lighting

The two groups were placed in separate pens in a basic open floor chicken pen with Aspen shaving bedding. We used trough-style feeders so that there was sufficient feeder space to ensure uniform access to the feed for each animal. During the first 2 days the pen had 24 h of constant light. We followed a standard lighting schedule modified from Schwean-Lardner et al. (2012) with constant lighting until day 3, when the lighting was reduced to 23 h of light and 1 h dark, with the amount of light decreasing each day until day 8, when the pen had 18 h of light and 6 h of dark. This level of lighting was maintained until the end of the study.

Feed restriction

We used a feed-restriction experimental design based on Williams et al. (2004) with a control group and a restricted group. The control group was fed *ad libidum* with a commercial chicken feed. The experimental group had their feed restricted to 50% of that consumed by the control group. The restricted diet was based on the previous day's *ad libitum* consumption, obtained by weighing the feed every morning. Following Williams et al. (2004), the restricted group was fed a custom feed with double the calcium and phosphorus content of the *ad libitum* feed, to maintain similar calcium and phosphorus intake at the 50% feed level. Our feed was obtained from the Canadian Feed Research Centre in North Battleford, Canada. This degree of restriction has been shown to permit normal growth and health in the animals, while producing a noticeable effect on gross bone morphology (Williams et al. 2004). For the first 4 days, both groups were fed *ad libitum* using a standard broiler starter feed. This ensured that feed restriction only occurred after the chicks were growing and developing normally.

Growth measurement

Each animal was wing-banded on day 1 and individually weighed daily to establish growth rates for both the control and restricted feed groups. Final total weight was also measured for each bird. We used weight to measure growth because it correlates strongly with major physiological traits (Blueweiss et al. 1978) and is easy to measure consistently across the short lifespan of the animals (Lee et al. 2013).

Sample preparation

The animals were euthanized after 42 days using a T-61 euthanasia solution injected into the brachial (wing) vein. The humeri and femora were dissected out from each bird and macerated to clean the bones to create better quality micro-CT images. We used warm water enzyme maceration, as it has been shown to be efficient while working on a short time scale while retaining good preservation. We used bromelain as our enzyme and Palmolive dish detergent as the active degreaser in an 80 °C water bath (Steadman et al. 2006; Lee et al. 2010). Before maceration we removed as much soft tissue from the bones as possible. We also used a magnetic stirrer to help loosen the remaining soft tissue from the bone during maceration.

Micro-CT

We used in-line phase contrast synchrotron micro-CT (Tafforeau et al. 2006; Betz et al. 2007; Cooper et al. 2011) to image the right humerus and femur from each individual animal at midshaft. We defined midshaft as 50% of the bone's maximum length. Micro-CT imaging was performed at the BioMedical Imaging and Therapy (BMIT) insertion device beamline (Wysokinski et al. 2015), part of the Canadian Light Source (CLS) synchrotron facility. We used a Hamamatsu C9300-124 optical camera paired with a Hamamatsu A40 X-ray converter for an effective pixel size of 4.3 μm at 32 keV. Each bone was scanned with exposure times between 0.7 and 1 s per projection, with 1500 projections for each scan, a total individual scan time of 20–30 min. The exact exposure time was chosen based on the synchrotron beam ring current, which decays from a peak of 250 mA over time. Flat and dark images were collected before each scan to correct for noise in the X-ray beam and the detector. An aluminum filter with an effective thickness of 1.1 mm was used to eliminate stray low energy harmonics in the X-ray beam. We used a propagation distance of 50 cm to optimize the phase in the scans (Pratt et al. 2015). Micro-CT at this resolution is able to distinguish canal microstructure (Cooper et al. 2007; Palacio-Mancheno et al. 2013), and phase contrast helps visualize microstructures and has a resolution enhancing effect (Pratt et al. 2015).

Image processing

We measured the orientation of the cortical network independently for each animal's humerus and femur scan following Pratt & Cooper (2017) and Pratt et al. (2018). We used a custom image processing software package developed using the IMAGEJ (ImageJ, NIH) scripting platform to perform most of the data processing. The script suite is available at https://github.com/isaacpratt/canal-orientation. We did our correction for detector and beam noise using flat and dark projections, and reconstructed the micro-CT projections using NRECON (Bruker SkyScan, Kontich BE), a commercial software package. We used AMIRA (FEI Company, USA) to extract and skeletonize the canal network from the micro-CT bone scans into a lineset format. The produced lineset file contains a series of points representing the central axis of each canal. From this we simplified the series of points into a set of line segments which we can measure the orientation of and which preserve the variability of orientation in the network. This lineset is then simplified into a series of line segments with a branch length set by the macro. We measured two angles for each line

segment: theta and phi. Phi is the angle between a canal segment and the long axis of the bone, and determines how longitudinal a canal is. Theta is the angle between a canal and a line from the bone centroid to the midpoint of that canal. The theta angle differentiates radial and circumferential canals. Using these two angles we can classify each line segment as longitudinal, radial, circumferential or oblique. We classified canal segments following de Margerie (2002) and Pratt & Cooper (2017). We then calculate three indices, a laminar index, a longitudinal index, and a radial index, as the ratio of the sum of the length of all the circumferential, longitudinal, or radial canal segments over the total length of all canal segments.

Statistical analysis

Statistical analysis was performed with SPSS version 24 (IBM, USA) using repeated measures two-way ANOVAs to compare simultaneously the three orientation indices between the two groups (between-subject factor) and the two bones (within-subject factor). We used pairwise comparisons to obtain the mean differences of the indices between the two groups and the two bones. Bodyweight and growth rate were compared using a repeated measures ANOVA. Sphericity was not rejected for our data. A Shapiro–Wilks test was run on all variables and all were found to be normally distributed. A Levene's test was run for all variables and homogeneity was not rejected. We set our alpha level at $P = 0.05$.

Results

At the end of the study (42 days) the mean weight of the control group, at 3366 g, was almost twice the mean weight of the restricted group, at 1698 g. The two groups started to diverge in weight at day 8 (restricted = 168.3 g; control = 185.3 g; $P = 0.049$) and the weight difference accelerated from there (see Fig. 1). Our broilers achieved higher final weights than those in Williams et al. (2004), with their 'commercial' strain (equivalent to our control group) achieving a weight of 2556 g and their restricted group achieving a weight of 1226 g. The final absolute growth rate of the control group at 42 days was 142.9 g day^{-1}, almost three times that of the restricted group, at 47.9 g day^{-1}. The two groups started to differ in absolute growth rate at day 6 (restricted = 18.2 g day^{-1}, control = 21.6 g day^{-1}, $P = 0.001$) and continued to diverge thereafter (see Fig. 2) although there were still some days after that where the difference in absolute growth rate was not significant (day 7, 11, 15).

Descriptive statistics for the laminar, radial, and longitudinal indices are shown in Table 1. Comparisons between groups and bones are shown in Tables 2 and 3, and P-values for all comparisons are shown in the tables. Statistics for the comparison between the restricted and control groups are shown in Table 2, and for the comparison between the humerus and femur in Table 3. The comparisons are illustrated in Fig. 3. Micro-CT slices are shown in Fig. 4 to show the microstructure and 3D renders of canal segments are shown in Fig. 5 to illustrate the orientations discussed in the text.

Both groups had very highly vascularized bones (see Fig. 4), with sections of new bone growth at the periosteum and endosteum. Larger vascular spaces were often seen close to the endosteal border of the bones, and long radial canals were often seen reaching far into the cortex from both the periosteal and endosteal borders. Typically the birds had larger femora than humeri. The most common canal type in the bones was radial for both groups' femora and the control humeri, and longitudinal for the restricted humeri. Several bones had areas, especially close to the periosteum, with locally higher numbers of circumferential canals near the periosteum but overall, the circumferential canal type was the least common for both bones in both groups.

We found that the laminar index was higher in the restricted group than in the control group for both bones, and higher in the humerus than the femur for both groups. The radial index was lower in the restricted group than in the control group for both bones, and lower in the humerus than in the femur for both groups. The longitudinal index was higher in the restricted group than in the control group for both bones, and higher in the humerus than the femur for both groups. No interaction effect was found between bone and group.

Discussion

Both the humerus and the femur in our study had areas of cortex with noticeably radial canals in both groups, although this was more evident in the femur and the control group. This was confirmed by the orientation index analysis, where the control group had a significantly higher radial index compared with the restricted group, and the femur a significantly higher radial index compared with the humerus. This aligns with previous research indicating that bone with radial canals has a higher growth rate than bone with other canal types (de Margerie et al. 2004). de Margerie et al. (2004) used fluorescent labeling in king penguin chicks and showed that bone with mainly radial vascularization had the fastest growth rate, followed by longitudinal and reticular (oblique) bone, and laminar bone with the slowest growth rate. Our results agree with this; our faster growing control group had a lower laminar index than the slower growing restricted group. Our results support the hypothesis that growth rate is linked to canal orientation and specifically that there is a connection between radial canals and faster growing bone. While the restricted group had a higher longitudinal index, the mean difference between the groups was slight, only 2.75 and 5.35% in the humerus and femur, respectively. The mean difference between the bones was much greater at 9.69 and 12.29% in the control and restricted groups respectively, with the longitudinal index significantly higher in the humerus than the femur. de Margerie et al. (2002) set 50% as the value of the laminar index required for calling a bone 'laminar' and
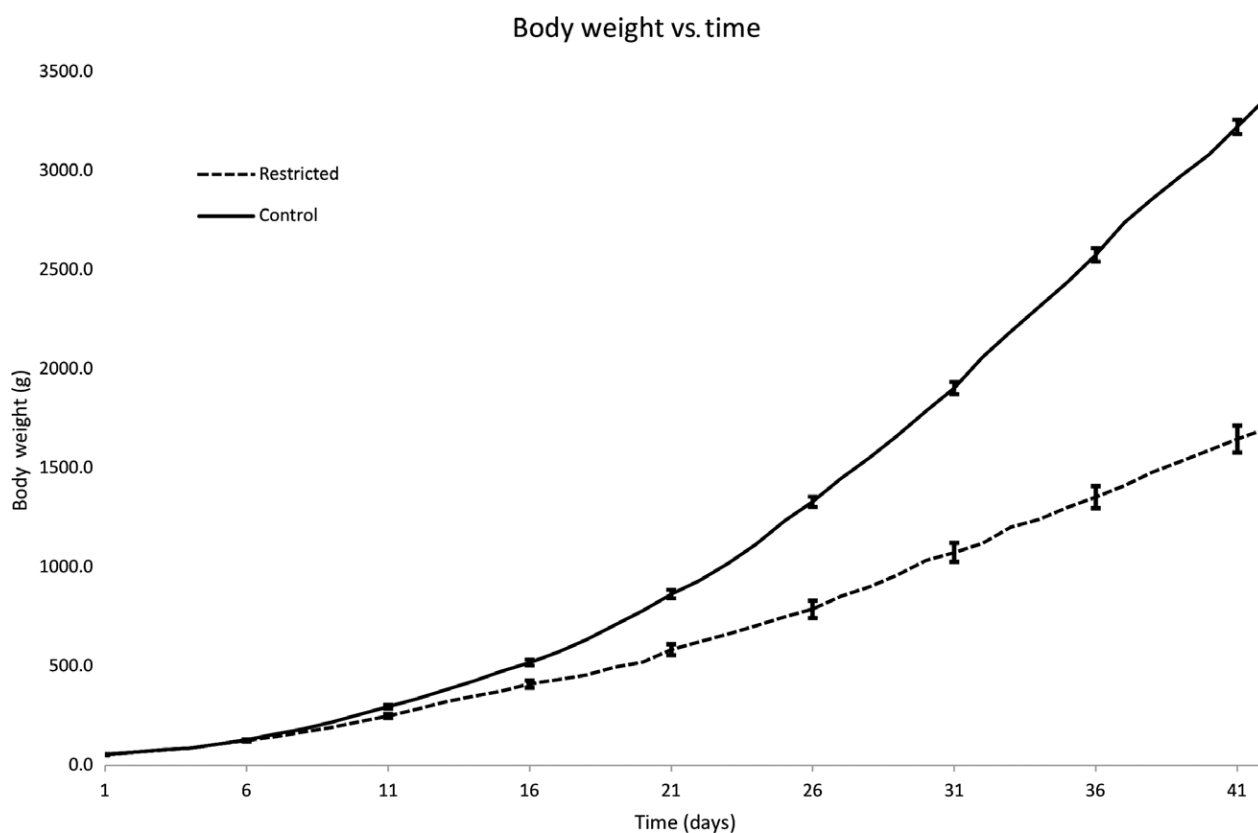
Body weight vs. time

Fig. 1 Mean bodyweight over time. The restricted group is shown with a dashed line and the control group with a solid line. Error bars show the standard error every five data points.

none of our bones met that value, although that value was for measurements from traditional histological sections, an approach which tends to overestimate the laminar index (Pratt et al. 2018). We found a significantly higher laminar index in the humerus than in the femur for our groups, supporting the functional loading hypothesis. These results conflict with the results found in our previous study (Pratt et al. 2018), where we found that the femur had a higher laminar index compared with the humerus. In that study we measured orientation indices in a broad 'comparative' sample of medium-large sized wild birds using the same method employed here.

A closer look at the data reported here shows that the laminar indexes for the humeri of the broiler group (15.64 ± 2.98% control and 21.60 ± 3.95% restricted) are in the same range as the laminar indices reported for the comparative bird group (18.3 ± 5.3%) presented in Pratt et al. (2018), whereas the laminar index for the broiler femora (10.02 ± 2.56% control and 14.54 ± 2.92% restricted) are lower than the femora of the comparative birds (23.2 ± 7.5%). The reason for the difference between the results presented here and our previous study is therefore likely to lie in biomechanical differences in the femur between broiler chickens and other bird species. Carrano (1998) measured a number of biomechanical properties in

hindlimbs of birds, including femur angle relative to the horizontal. They found that chickens had the most vertical orientation of all the extant birds they sampled. In a later study involving experimental alteration of limb posture, Carrano & Biewener (1999) found that chickens with more horizontal femur angles experienced less torsional force compared with chickens with more vertical femur angles. This suggests that the femora in our chickens likely experience lower torsional force than the femora of the comparative bird sample from Pratt et al. (2018), explaining why we found different patterns in the laminar index in this study. Broiler chickens can fly only limited distances in short bursts and the restricted group exhibited more flying behavior in the open pen than did the control group, likely as a consequence of the higher weight of control group. The limited use of their wings means they are likely to experience less torsional stress on the bones compared with the more intensely flying birds in the Pratt et al. (2018) study. Based on this, the higher laminar index we found in the restricted group than in the control group may support the functional loading hypothesis. It could also be that the higher laminar index in the humerus than the femur is due to a lower growth rate in the humerus. Overall, our results support interpreting the orientation of vascular canals as a response to both growth rate and functional loading.

Absolute growth rate over time
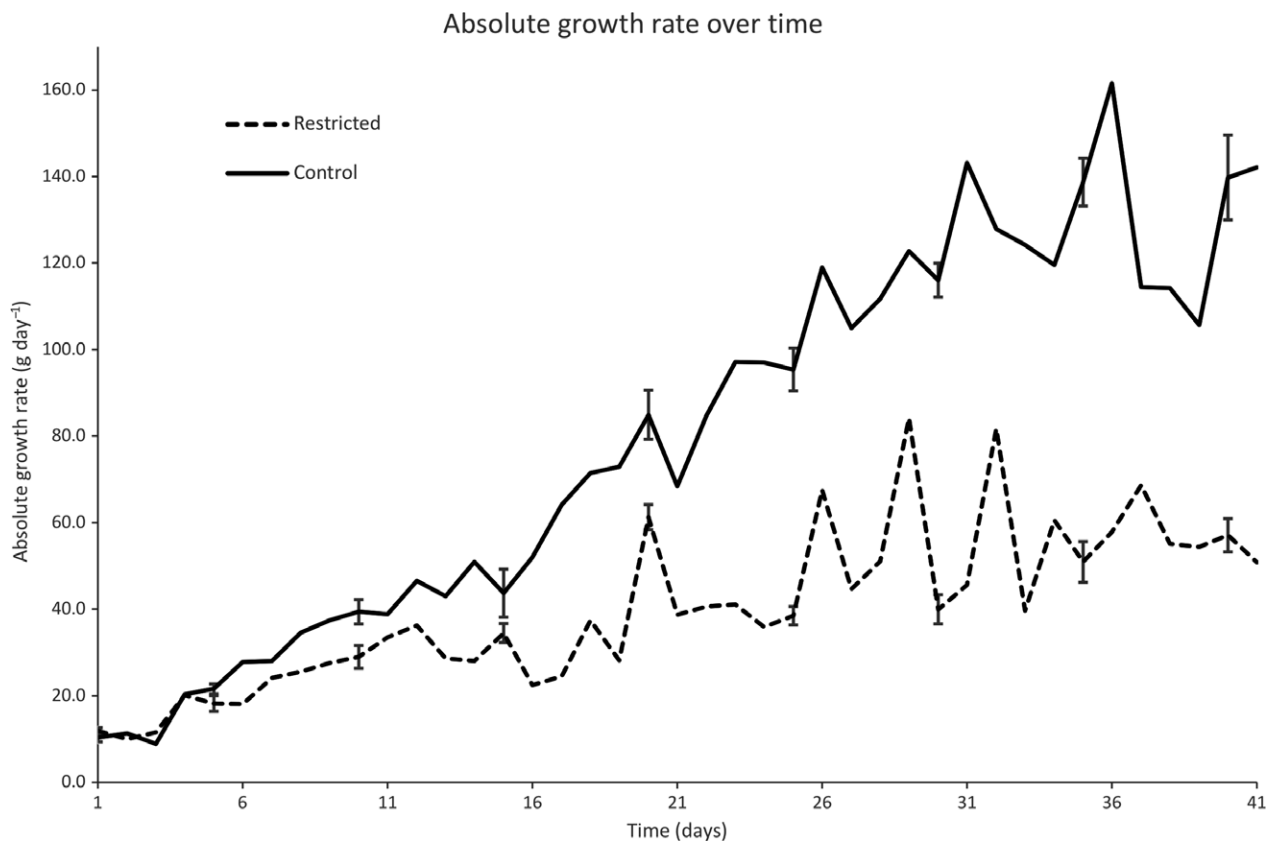
Fig. 2 Mean growth rate over time. The restricted group is shown with a dashed line and the control group with a solid line. Error bars show the standard error every five data points.

Table 1 Descriptive statistics for the cortical orientation indices.

Variable	Study group	Bone	Mean (%)	SD (%)
Laminar index	Control	Humerus	15.64	2.98
		Femur	10.02	2.56
	Restricted	Humerus	21.60	3.95
		Femur	14.54	2.92
Radial index	Control	Humerus	38.71	5.46
		Femur	55.64	5.37
	Restricted	Humerus	28.75	3.81
		Femur	44.44	4.37
Longitudinal index	Control	Humerus	33.46	3.46
		Femur	21.17	3.12
	Restricted	Humerus	36.21	2.98
		Femur	26.52	3.95

Table 2 Comparison between control and restricted chicken groups. A positive mean difference means the control group has a higher value than the restricted group. All variables were found to be statistically significant.

Variable	Bone	Mean difference (%)	SE	Significance
Laminar index	Humerus	−5.96	1.21	<0.001
	Femur	−4.51	0.95	<0.001
Radial index	Humerus	9.96	1.65	<0.001
	Femur	11.21	1.71	<0.001
Longitudinal index	Humerus	−2.75	1.13	0.021
	Femur	−5.35	1.23	<0.001

We used bodyweight as a proxy for bone growth, as measuring bone growth directly is complex. Jepsen & Andarawis-Puri (2012) built a model of human bone apposition during aging and found that differences in cortical thickness and diameter affected the apposition rate of bone. In particular, through their simulation they found that slender bones needed to have a higher periosteal apposition rate compared with more robust bones to maintain stiffness during aging. This paper points out that bone growth and bone modeling are not constant or necessarily consistent. The result is that bone growth may not be linear and/or equivalent within each of our animal groups or bones. While this proxy is sufficient for our analysis, further studies could add new information by measuring bone growth directly. Potential methods to measure bone formation rate include fluorochrome labeling, although it is invasive and not always reliable (de Margerie et al. 2004); using cross-

Table 3 Comparison between humerus and femur in the control and restricted chicken groups. A positive mean difference means the humerus has a higher average value than the femur. All variables were found to be statistically significant.

Variable	Group	Mean difference (%)	SE	Significance
Laminar index	Control	5.62	1.02	<0.001
	Restricted	7.06	1.05	<0.001
Radial index	Control	−16.94	1.51	<0.001
	Restricted	−15.69	1.56	<0.001
Longitudinal index	Control	12.29	1.07	<0.001
	Restricted	9.69	1.10	<0.001

sectional bone geometry data to produce general bone growth curves, which requires more animals, and using longitudinal *in vivo* micro-CT, which can measure changes in cortical diameter.

Birds go through remodeling throughout their lifespan, so if the orientation of secondary canals produced after flight behavior manifests differently from the orientation of the primary canals, that change could be shown using a longitudinal study and might reflect changes in locomotor behavior or changes in growth rate in mature bone tissue. Along those lines, Skedros & Hunt (2004) measured the laminar index in turkey ulnae and found that adults had a significantly higher laminar index compared with sub-adults. They proposed two possible interpretations: either a link to a mechanical/functional loading change in adulthood or a change in growth rate. Their mechanical hypothesis was based on either the primary vascular network being linked to a prevalent strain direction and primary bone laid down around it or the collagen fiber orientation being linked to the strain direction directly and mediating the orientation

of the vascular canal network. Their second hypothesis is based on ontogenic changes in growth rate, following Lee (2004) and Petrtyl et al. (1996), who propose that a greater longitudinal orientation of canals in primary bone aligns with a greater bone growth direction in that direction. They suggest that a prevalence of longitudinal canals is a consequence of longitudinal shifting of the periosteum against the bone surface.

Measuring laminar and other indices using histology underestimates the number of longitudinal canals present in a bone section. The method popularized by de Margerie et al. (2002) uses the area of the canals to calculate the laminar index, and because most of the area of longitudinal canals is perpendicular to the cross-section, it is consistently underestimated. Our previous work (Pratt et al. 2018) using the same technique has shown that using an area-based index measurement underestimated the area of longitudinal canals by 20% and consequentially overestimate the laminar index by 7.7% in a comparative sample of birds and bats. The conventional criteria for assigning a canal as longitudinal is based on a measurement of how circular the cross section of the canal is in the plane of sectioning, which relies on the assumption that canals are circular (de Margerie, 2002; de Boef & Larsson, 2007). Our experience, along with evidence from micro-CT, suggests that this assumption is not consistently well supported (Hennig et al. 2015), and that osteons and canals are not always circular in cross-section but often oval in shape.

We believe that micro-CT is the ideal method for measuring canal orientation as it measures the complete cortical network in 3D, easily capturing data for a large proportion of a long bone shaft. It does, however, have a lower resolution than histology, and lab-based micro-CT systems are typically unable to visualize some histological features of interest including canaliculi, lines of arrested growth (LAGs),
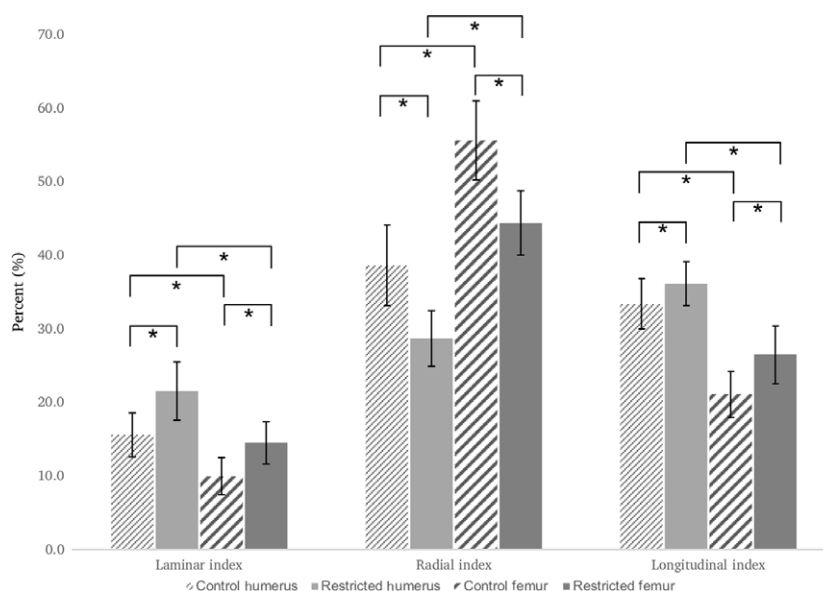
Fig. 3 Graph showing the comparison of the laminar, radial, and longitudinal indices between the humerus and femur in the control and restricted groups. Error bars show the standard error and significant differences are marked with an asterisk.
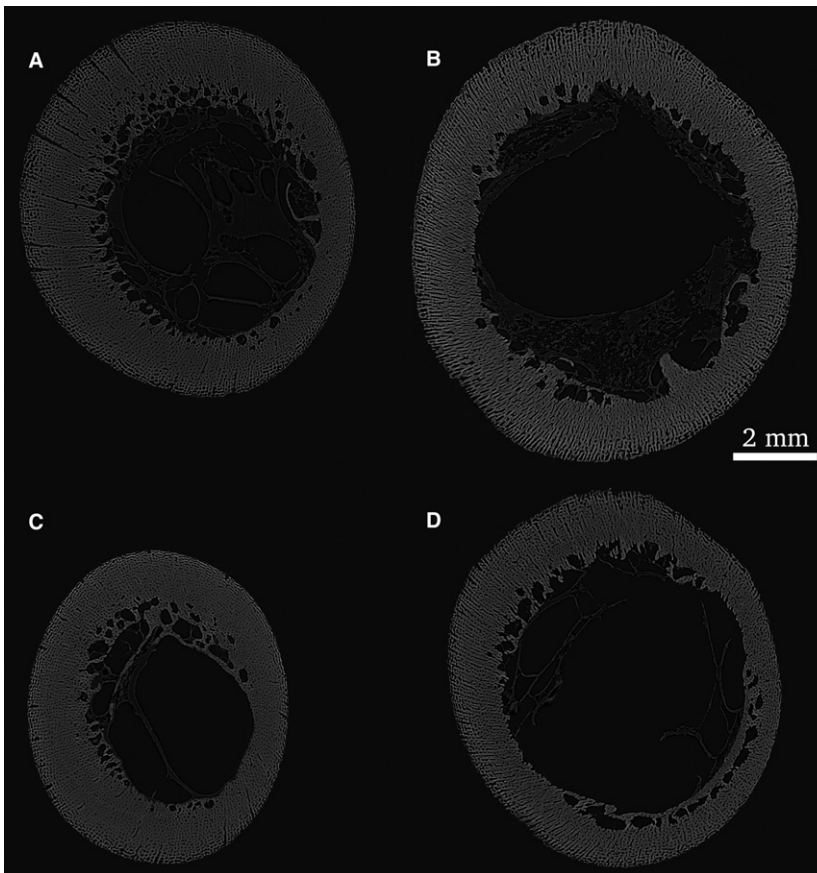
Fig. 4 Micro-CT slices. Each image is created by averaging five consecutive micro-CT slices. (A) Control humerus, (B) control femur, (C) restricted humerus, and (D) a restricted femur. All the images are of 42-day-old animals post-euthanization. Several radial canals are noticeable in the top left of (A).

and osteonal boundaries (Cooper et al. 2011). These resolution deficiencies can be remedied with advanced nano-CT (Peyrin et al. 2014) or phase contrast enhanced micro-CT systems (Arhatari et al. 2011; Cooper et al. 2011; Sanchez et al. 2012; Carter et al. 2013; Andronowski et al. 2017) that have resolutions higher than 1–2 μm, but these systems are rare and expensive.

Based on the quality of the micro-CT scans in this study we were unable to differentiate primary canals and secondary canals. For our animals because of their short lifespan we can assume that all the canals are from their current growth period/functional loading regime and will be predominantly primary, but distinguishing primary from secondary canals can be very important in longitudinal studies or studies of animals later in life. With higher resolution phase contrast micro-CT with resolution around or better than 1–2 μm, it is possible to visualize osteon boundaries and distinguish these canal types (Arhatari et al. 2011; Maggiano et al. 2016) and this level of resolution could add new information if used in future studies. Previous research has shown that *in vivo* micro-CT can be used to image cortical canals in live rats (Harrison & Cooper, 2015; Pratt et al. 2015), using phase contrast to overcome the necessity of low dose. This technique could be used for longitudinal experimental studies modifying the behavior or growth rate of an animal.

Conclusion

We found a higher growth rate, a higher radial index, and a lower laminar index in the control group than in the restricted group. These results support the hypothesis that vascular canal orientation is connected to growth rate, with radial canals linked to faster growth and circumferential canals (and laminar index) to slower growth. We also found a higher laminar index in the humerus than in the femur, supporting the hypothesis that canal orientation is linked to functional loading – specifically, a high laminar index is linked to torsional loading. Overall, our results indicate that a complex interplay of growth rate and functional loading determines the predominant orientation of the cortical canal network. Experimental studies on animal models are a useful tool for investigating cortical bone microstructure. Further experiments should look at conducting longitudinal studies using *in vivo* scanning to investigate the time period around the transition to adulthood. This period often includes changes to locomotor behavior such as the acquisition of flight in birds or changes in growth rate due to the acquisition of adult body weight. Mechanical testing of specific bone sections with different canal types could also add information about potential differences in directional bone strength.
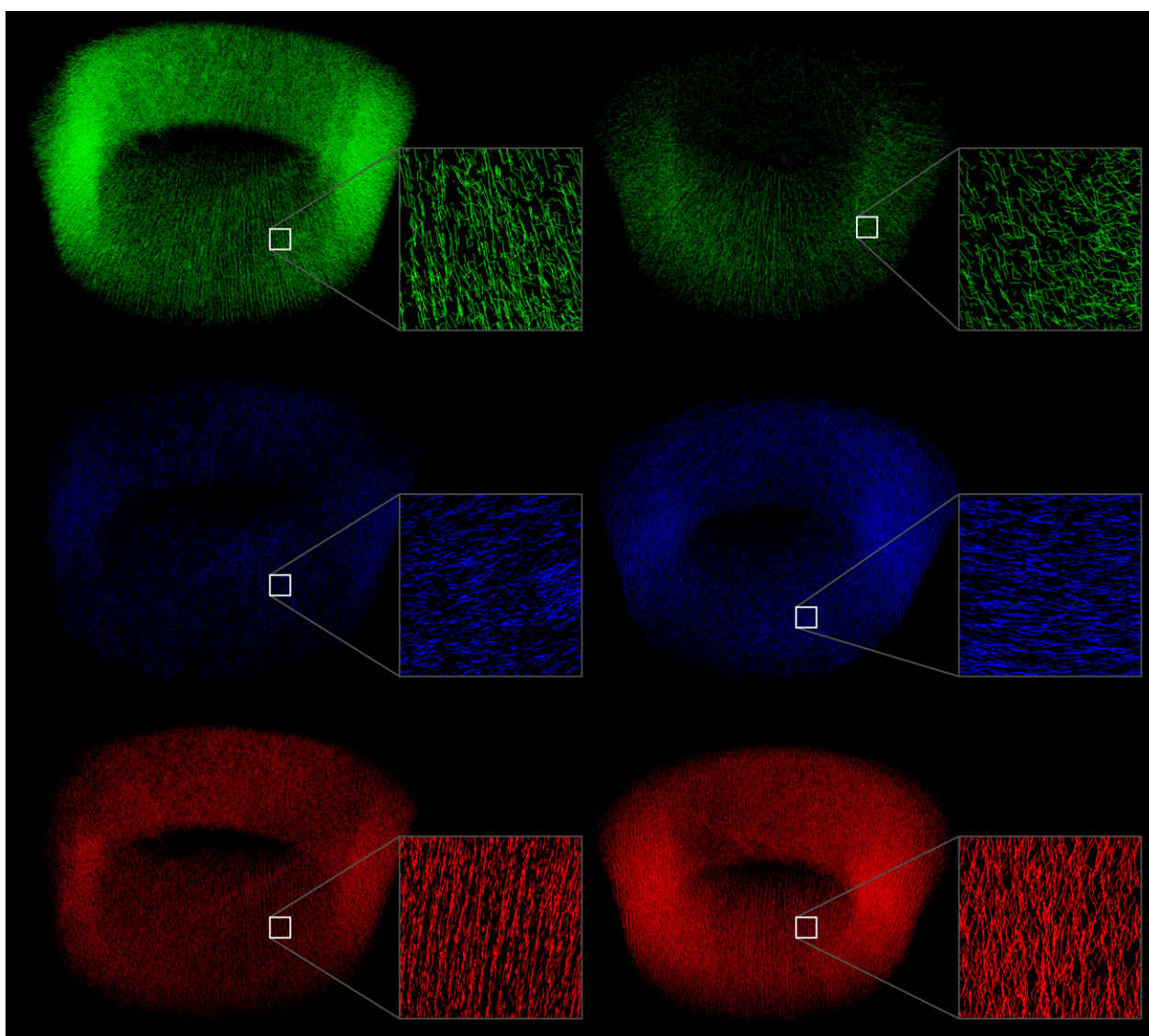
Fig. 5 3D renders of canal segments with circumferential shown in blue, longitudinal in red, and radial in green. The left side shows a control femur with a high radial index and a low laminar index. The right side shows a restricted humerus with a low radial index and a high laminar index. Inset panes show close-ups of the canals to better show the orientation. All the images are of 42-day-old animals post-euthanization.

References

Ammann P, Rizzoli P (2003) Bone strength and its determinants. *Osteoporos Int* **14**(Suppl 3), S13–S18.

Andronowski JM, Pratt IV, Cooper DML (2017) Occurrence of osteon banding in adult human cortical bone. *Am J Phys Anthropol* **28**, 211–642.

Arhatari BD, Cooper DML, Thomas CDL, et al. (2011) Imaging the 3D structure of secondary osteons in human cortical bone using phase-retrieval tomography. *Phys Med Biol* **56**, 5265–5274.

Betz O, Wegst U, Weide D, et al. (2007) Imaging applications of synchrotron X-ray phase-contrast microtomography in biological morphology and biomaterials science. 1. General aspects of the technique and its advantages in the analysis of millimetre-sized arthropod structure. *J Microsc* **227**, 51–71.

Blueweiss L, Fox H, Kudzma V, et al. (1978) Relationships between body size and some life history parameters. *Oecologia* **37**, 257–272.

De Boef M, Larsson HCE (2007) Bone microstructure: quantifying bone vascular orientation. *Can J Zool* **85**, 63–70.

De Boef M, Larsson H, Horner J (2007) Measurements of vasculature in *Tyrannosaurus rex* show a relationship between growth rate and vasculature orientation. *J Vertebrate Paleontol* **27**, 67A.

Britz HM, Jokihaara J, Leppänen OV, et al. (2012) The effects of immobilization on vascular canal orientation in rat cortical bone. *J Anat* **220**, 67–76.

Carrano MT (1998) Locomotion in non-avian dinosaurs: integrating data from hindlimb kinematics, in vivo strains, and bone morphology. *Paleobiology* **24**, 450–469.

Carrano MT, Biewener AA (1999) Experimental alteration of limb posture in the chicken (*Gallus gallus*) and its bearing on the use of birds as analogs for dinosaur locomotion. *J Morphol* **240**, 237–249.

Carter Y, Thomas CDL, Clement JG, et al. (2013) Variation in osteocyte lacunar morphology and density in the human femur – a synchrotron radiation micro-CT study. *Bone* **52**, 126–132.

Cooper DML, Turinsky AL, Sensen CW, et al. (2003) Quantitative 3D analysis of the canal network in cortical bone by micro-computed tomography. *Anat Rec B New Anat* **274**, 169–179.

Cooper D, Turinsky A, Sensen C, et al. (2007) Effect of voxel size on 3D micro-CT analysis of cortical bone porosity. *Calcif Tissue Int* **80**, 211–219.

Cooper DML, Erickson B, Peele AG, et al. (2011) Visualization of 3D osteon morphology by synchrotron radiation micro-CT. *J Anat* **219**, 481–489.

Cooper DML, Kawalilak CE, Harrison K, et al. (2016) Cortical bone porosity: what is it, why is it important, and how can we detect it? *Curr Osteoporos Rep* **14**, 187–198.

Currey JD (2002) *Bones: Structure and Mechanics*. Princeton: Princeton University Press.

Harrison KD, Cooper D (2015) Modalities for visualization of cortical bone remodeling: the past, present, and future. *Front Endocrinol (Lausanne)* **6**, 122.

Hennig C, Thomas CDL, Clement JG, et al. (2015) Does 3D orientation account for variation in osteon morphology assessed by 2D histology? *J Anat* **227**, 497–505.

Hert J, Fiala P, Petrtyl M (1994) Osteon orientation of the diaphysis of the long bones in man. *Bone* **15**, 269–277.

Jepsen KJ, Andarawis-Puri N (2012) The amount of periosteal apposition required to maintain bone strength during aging depends on adult bone morphology and tissue-modulus degradation rate. *J Bone Miner Res* **27**, 1916–1926.

Knowles TG, Kestin SC, Haslam SM, et al. (2008) Leg disorders in broiler chickens: prevalence, risk factors and prevention. *PLoS ONE* **3**, e1545.

Lee AH (2004) Histological organization and its relationship to function in the femur of *Alligator mississippiensis*. *J Anat* **204**, 197–207.

Lee EJ, Luedtke JG, Allison JL, et al. (2010) The effects of different maceration techniques on nuclear DNA amplification using human bone. *J Forensic Sci* **55**, 1032–1038.

Lee AH, Huttenlocker AK, Padian K, et al. (2013) Analysis of growth rates. In *Bone Histology of Fossil Tetrapods*. , pp. 216–251, Berkeley: University of California Press.

Leterrier C, Nys Y (1992) Composition, cortical structure and mechanical properties of chicken tibiotarsi: effect of growth rate. *Br Poult Sci* **33**, 925–939.

Maggiano CM (2012) Making the mold: a microstructural perspective on bone modeling during growth and mechanical adaptation. In: *Bone Histology: An Anthropological Perspective*. (eds Crowder C, Stout S), pp. 45–90, Boca Raton: CRC Press.

Maggiano IS, Maggiano CM, Clement JG, et al. (2016) Three-dimensional reconstruction of Haversian systems in human cortical bone using synchrotron radiation-based micro-CT: morphology and quantification of branching and transverse connections across age. *J Anat* **228**, 719–732.

de Margerie E (2002) Laminar bone as an adaptation to torsional loads in flapping flight. *J Anat* **201**, 521–526.

de Margerie E, Cubo J, Castanet J (2002) Bone typology and growth rate: testing and quantifying 'Amprino's rule' in the mallard (*Anas platyrhynchos*). *C R Biol* **325**, 221–230.

de Margerie E, Robin JP, Verrier D, et al. (2004) Assessing a relationship between bone microstructure and growth rate: a fluorescent labelling study in the king penguin chick (*Aptenodytes patagonicus*). *J Exp Biol* **207**, 869–879.

Palacio-Mancheno PE, Larriera AI, Doty SB, et al. (2013) 3D assessment of cortical bone porosity and tissue mineral density using high-resolution μCT: effects of resolution and threshold method. *J Bone Miner Res* **29**, 142–150.

Petrtyl M, Hert J, Fiala P (1996) Spatial organization of the haversian bone in man. *J Biomech* **29**, 161–169.

Peyrin F, Dong P, Pacureanu A, et al. (2014) Micro- and nano-CT for the study of bone ultrastructure. *Curr Osteoporos Rep* **12**, 465–474.

Pines M, Reshef R (2014) Poultry Bone Development and Bone Disorders. In: *Sturkie's Avian Physiology: Sixth Edition*: pp. 367–377. London, England: Elsevier.

Pratt IV, Cooper DML (2017) A method for measuring the three-dimensional orientation of cortical canals with implications for comparative analysis of bone microstructure in vertebrates. *Micron* **92**, 32–38.

Pratt IV, Belev G, Zhu N, et al. (2015) In vivo imaging of rat cortical bone porosity by synchrotron phase contrast micro computed tomography. *Phys Med Biol* **60**, 211–232.

Pratt IV, Johnston JD, Walker E, et al. (2018) Interpreting the three-dimensional orientation of vascular canals and cross-sectional geometry of cortical bone in birds and bats. *J Anat* **14**, S13.

Rawlinson SCF, Murray DH, Mosley JR, et al. (2009) Genetic selection for fast growth generates bone architecture characterised by enhanced periosteal expansion and limited consolidation of the cortices but a diminution in the early responses to mechanical loading. *Bone* **45**, 357–366.

de Ricqlès AJ, Meunier F, Castanet J, et al. (1991) Comparative microstructure of bone. *Bone* **3**, 1–78.

Sanchez S, Ahlberg PE, Trinajstic KM, et al. (2012) Three-dimensional synchrotron virtual paleohistology: a new insight into the world of fossil bone microstructures. *Microsc Microanal* **18**, 1095.

Schwean-Lardner K, Fancher BI, Classen HL (2012) Impact of daylength on the productivity of two commercial broiler strains. *Br Poult Sci* **53**, 7–18.

Shim MY, Karnuah AB, Mitchell AD, et al. (2012) The effects of growth rate on leg morphology and tibia breaking strength, mineral density, mineral content, and bone ash in broilers. *Poult Sci* **91**, 1790–1795.

Skedros JG, Hunt KJ (2004) Does the degree of laminarity correlate with site-specific differences in collagen fibre orientation in primary bone? An evaluation in the turkey ulna diaphysis. *J Anat* **205**, 121–134.

Steadman DW, DiAntonio LL, Wilson JJ, et al. (2006) The effects of chemical and heat maceration techniques on the recovery of nuclear and mitochondrial DNA from bone. *J Forensic Sci* **51**, 11–17.

Tafforeau P, Boistel R, Boller E, et al. (2006) Applications of X-ray synchrotron microtomography for non-destructive 3D studies of paleontological specimens. *Appl Phys A Mater Sci Process* **83**, 195–202.

Williams B, Solomon S, Waddington D, et al. (2000) Skeletal development in the meat-type chicken. *Br Poult Sci* **41**, 141–149.

Williams B, Waddington D, Murray DH, et al. (2004) Bone strength during growth: influence of growth rate on cortical porosity and mineralization. *Calcif Tissue Int* **74**, 236–245.

Wysokinski TW, Chapman D, Adams G, et al. (2015) Beamlines of the biomedical imaging and therapy facility at the Canadian light source – part 3. *J Phys Conf Ser* **775**, 1–4.